Eur Biophys J (2002) 30: 617–624
DOI 10.1007/s00249-001-0188-9

BIOPHYSICS LETTER

**Bernard Chasan · Nicholas A. Geisse · Kate Pedatella
David G. Wooster · Martin Teintze
Marcelo D. Carattino · Wolfgang H. Goldmann
Horacio F. Cantiello**

Evidence for direct interaction between actin and the cystic fibrosis transmembrane conductance regulator

Received: 28 May 2001 / Revised version: 27 August 2001 / Accepted: 7 September 2001 / Published online: 30 October 2001

Abstract Previous studies have demonstrated that actin filament organization controls the cystic fibrosis transmembrane conductance regulator (CFTR) ion channel function. The precise molecular nature of the interaction between actin and CFTR, however, remains largely unknown. In this report, interactions between actin and purified human epithelial CFTR were directly assessed by reconstitution of the channel protein in a lipid bilayer system and by atomic force microscopy (AFM). CFTR-containing liposomes in solution were deposited on freshly cleaved mica and imaging was performed in tapping-mode AFM. CFTR function was also determined in identical preparations. Images of single CFTR molecules were obtained, and addition of monomeric actin below its critical concentration showed the formation of actin filaments associated with CFTR. The data indicate a direct interaction between actin and CFTR exists, which may explain the regulatory role of the cytoskeleton in ion channel function. This was confirmed by functional studies of CFTR single-channel currents, which were regulated by addition of various conformations of actin. The present study indicates that CFTR may directly bind actin and that this interaction helps affect the functional properties of this channel protein.

Keywords Cytoskeleton · Ion channel reconstitution · Electrophysiology · Cystic fibrosis · Atomic force microscopy

W.H. Goldmann · H.F. Cantiello (✉)
Renal Unit, Massachusetts General Hospital East,
149 13th Street, Charlestown, MA 02129, USA
E-mail: cantiello@helix.mgh.harvard.edu
Tel.: +1-617-7265640
Fax: +1-617-7265669

B. Chasan · N.A. Geisse · K. Pedatella
Physics Department, Boston University,
Boston, MA, USA

D.G. Wooster · M. Teintze
Chemistry and Biochemistry Department,
Montana State University, Bozeman, MT, USA

M.D. Carattino · H.F. Cantiello
Laboratorio de Canales Iónicos,
Cátedra de Química General e Inorgánica,
Facultad de Farmacia y Bioquímica,
Buenos Aires, Argentina

W.H. Goldmann · H.F. Cantiello
Department of Medicine, Harvard Medical School,
Boston, MA, USA

Introduction

Previous studies from our laboratory (Prat et al. 1995, 1999) demonstrated a functional role for actin filament organization in the activation and regulation of the cystic fibrosis transmembrane conductance regulator (CFTR), the anion selective channel whose dysfunction leads to the onset of cystic fibrosis (Rich et al. 1990; Berger et al. 1991). In our original report, addition of either cytochalasin D to disrupt endogenous actin filaments, or addition of exogenous actin in the absence of protein kinase A (PKA), induced the activation of CFTR (Prat et al. 1995). Further, the collapse of the actin cytoskeleton by prolonged treatment with cytochalasin D completely prevented the activation of CFTR by the cAMP pathway. PKA-insensitive CFTR function could be readily restored by addition of exogenous actin. More recent studies indicate that three-dimensional actin networks, elicited by binding of the filamin homologue ABP-280 to actin filaments, are also required for a proper cAMP activation of CFTR (Prat et al. 1999). These findings suggest that CFTR interacts with actin, either directly (Prat et al. 1995) and/or in combination with actin-associated proteins (Short et al. 1998; Prat et al. 1999). The binding of actin to CFTR may be mediated by the actin-binding protein ezrin (Short et al. 1998). However, the molecular chaperone Hsc70, which is structurally related to actin (Hurley 1996), binds to the nucleotide binding domain of CFTR (Strickland et al. 1997), suggesting that actin itself may also directly

interact with the channel protein. To date, the nature of the interaction(s) between actin and CFTR is still undetermined.

In the present study, ion channel reconstitution showed a regulatory role of actin binding in CFTR function. A physical interaction between actin and CFTR was also determined by atomic force microscopy (AFM) in tapping mode (Binning et al. 1986; Drake et al. 1989). Imaging of single CFTR molecules was achieved in saline solution incorporated into flattened lipid bilayers. The data indicated that the exposed cytoplasmic domains of CFTR bind and likely facilitate actin polymerization. The study is, to our knowledge, the first imaging of cytoskeletal interactions with an ion channel in lipid membranes. The study supports the concept that actin directly interacts with CFTR to elicit ion channel regulation.

Materials and methods

Purification of CFTR

Recombinant human epithelial CFTR was obtained from baculovirus infected Sf9 insect cell membranes according to O'Riordan et al. (1995). Briefly, the human epithelial CFTR cDNA (a kind gift of Dr. Francis Collins) was transferred into a baculovirus vector (PVL1393, Invitrogen, San Diego, Calif.) for over-expression in Sf9 cells. Twelve 75 cm^2 flasks of Sf9 cells were grown to confluence and infected with baculovirus stock at approximately 5 MOI for 1 h. The virus was then removed and replaced by medium containing 10% fetal bovine serum (Sigma, St. Louis, Mo.), and cells were incubated 48–56 h post-infection. The cells were then harvested by pelleting at 800×*g* and then washed in phosphate buffer before repelleting. Each pellet was frozen at –70 °C until needed. At the time of purification, two pellets (i.e. two 75 cm^2 flasks) of cells were thawed and resuspended in 4 mL of alkaline extraction solution (10 mM NaOH, 0.1 mM EDTA), also containing the protease inhibitors leupeptin (50 μg/mL), aprotinin (50 μg/mL), and PMSF (100 μg/mL). The suspension was vortexed for 3 min. Cell membranes were pelleted by ultracentrifugation at 100,000×*g* for 40 min at 10 °C. The pellet was then re-suspended in 4 mL of buffer containing 10 mM sodium phosphate, 2% sodium dodecyl sulfate (SDS), and 0.5 mM dithiothreitol (DTT), pH 6.4. The sample was solubilized by periodically pipetting for 40–60 min at room temperature. CFTR was purified in a hydroxyapatite column (ceramic type II, BioRad, Richmond, Calif.) with a total volume bed of approximately 6 cm^3, which had been pre-equilibrated with a solution containing 10 mM phosphate, 0.5 mM DTT, and 0.15% SDS. Unbound proteins were washed off with more of the same buffer (~2 column volumes). Absorbance of each fraction was measured at 280 nm. A step gradient of phosphate buffer was then applied in the order (in mM) 300, 320, 360, 400, also with 0.15% SDS. CFTR co-eluted with a protein of lower molecular weight, which is believed to be a breakdown product at the 400 mM step. The CFTR-containing fractions were concentrated by centrifugation at 1000×*g* in Amicon Centricon 50 tubes (Amicon, Beverly, Mass.) to a volume of about 0.5 mL. The concentrate was then subjected to gel filtration using G-100–120 Sephadex beads (Sigma) in a column of 18 cm in height and 2 cm in diameter. The elution buffer contained 10 mM Tris, 100 mM NaCl, 0.25% lithium dodecyl sulfate (LiDS), pH 8.0. CFTR eluted in the first peak. Only the early parts of the peak were collected and reconcentrated using Centricon tubes to a final volume of 200 μL. This eluent was rediluted in 800 μL of a solution containing (in mM) HEPES (15) and EGTA (0.5), pH 7.2. The diluted eluent was reconcentrated to a final volume of 100–200 μL to be used for liposome reconstitution.

Reconstitution of CFTR into phospholipid vesicles

The reconstitution procedure of the CFTR-containing samples was as follows: a chloroform solution containing phosphatidylethanolamine (PE), phosphatidylserine (PS), and phosphatidylcholine (PC) (Avanti Polar Lipids, Alabaster, Ala.) in a 5:2:1 molar ratio was dried out under argon gas. The film was solubilized by sonication for 15 min, in a HEPES buffer containing (in mM) HEPES (15), EGTA (0.5), and 1% cholate, to a final lipid concentration of 10 mg/mL, pH 7.2. A 100 μL sample of sonicated lipids was then combined with the CFTR sample and incubated on ice for 40–60 min. The mixture was dialyzed for 24 h at 4 °C against 2 L of the HEPES buffer containing 1.5% cholate (Spectra/Por, MWCO 12–14,000), and followed by daily changes of 2 L of HEPES buffer without detergent for a total of 3 days. Proteoliposomes were then re-concentrated to a volume of 200 μL, and aliquoted and stored frozen at –70 °C.

Planar lipid bilayer studies

Functional reconstitution of CFTR was conducted in a lipid bilayer reconstitution system as recently reported (Cantiello et al. 1998). The reconstituted protein was either fused into the lipid bilayer by reconstitution of proteoliposomes with techniques previously described (Cantiello et al. 1998), or applied directly to the lipid bilayer after elution through a Sephadex G-50-fine column to remove denaturing SDS (Cantiello et al. 1998). Either proteoliposomes containing purified CFTR, or CFTR mixed with lipid components, were fused to planar lipid bilayers by painting onto a 0.1 mm hole in a 13 mm polystyrene cuvette (Warner Instrument, Hamden, Conn.), as described by Alvarez (1986). The phospholipid composition of the lipid bilayers was 7:2:1 (v/v) PE:PC:PS (Avanti Polar Lipids) in *n*-decane (Aldrich, Milwaukee, Wis.) to a final concentration of 14, 6, and 0.5 mM, respectively. The initial *cis* and *trans* solutions usually contained 10 mM MOPS, pH 7.4, and 10 and 100 mM MgATP, respectively.

Atomic force microscopy

A model 3000 AFM (Digital Instruments, Santa Barbara, Calif.), attached to a Nanoscope IIIa controller with an electronics extender box, was used for the present studies. Images were obtained with oxide-sharpened silicon nitride tips (DNP-S; Digital Instruments) mounted on thick (21 μm) and short (100 μm) cantilevers unless otherwise noted. Drive frequencies obtained with these cantilevers were typically in the range of 7.9–8.2 kHz. Samples were deposited onto freshly cleaved mica disks mounted onto either glass slides or magnetic circular pucks. All scans were conducted in aqueous solution. Images were flattened to a zeroth- or first-order polynomial fit, and no further filtering or data modification were performed.

CFTR-containing liposomes in buffer were deposited on freshly cleaved mica and allowed to flatten onto the mica, forming extended bilayers. Initially, liposomes were left on the mica for 2 h at 37 °C prior to scanning. However, most studies were conducted with liposomes incubated at room temperature for a 15 min period, with similar results. Care was taken to keep the buffer from evaporating during incubation. Samples were sealed into a Petri dish, which was kept humidified by a wet paper towel. Samples were scanned in solution by adding sufficient buffer to form a meniscus between tip and sample. Typically, total liquid volumes of 100 μL were used. When necessary, small volumes of order 2–10 μL were added without serious perturbation. Unless otherwise indicated, imaging was carried out in an actin depolymerizing (G) buffer, containing 0.2 mM $CaCl_2$, 0.2 mM MgATP, 0.2 mM β-mercaptoethanol, and 2 mM tris(hydroxymethyl)aminomethane-HCl (Tris-HCl, pH 8.0).

Single-channel recordings of reconstituted CFTR

Input signals were acquired with a PC-501A patch/whole cell clamp amplifier via a 10 GΩ head-stage for lipid bilayers (Warner

Instrument, Hamden, Conn.). The output currents were low-pass filtered at 500 Hz with an eight-pole Bessel filter (Frequency Devices, Haverill, Mass.). Signals were digitized at 37 kHz and 14-bits with a VR-10B digital data recorder (Instrutech, Great Neck, NY), and stored on a video cassette recorder (JVC, Fairfield, NJ). Further analysis was conducted with PClamp 6.0.3 (Axon Instruments, Foster City, Calif.). Single-channel tracings were Gaussian-filtered at 100–200 Hz for display purposes, and analyzed as previously reported (Cantiello et al. 1998). The single-channel conductance of functional CFTR under asymmetrical ATP and ATP/Cl conditions was obtained by fitting experimental current values at different holding potentials to the Goldman-Hodgkin-Katz (GHK) equation, as previously described (Cantiello et al. 1998).

Calculations

Calculations of the perm-selectivity ratios under either asymmetrical MgATP (10/100 mM) or ATP/Cl conditions were obtained from current-to-voltage relationships as recently reported (Cantiello et al. 1998), such that single-channel conductances [current (I) divided by holding potential, V_h] were best fitted to the GHK equation:

$$I(V_h) = (z_i^2 F^2 P_i V_h/RT)\{C_c/[1-\exp(-\alpha)]\} + \left(z_j^2 F^2 P_j V_h/RT\right)\{C_t/[1-\exp(+\beta)]\} \quad (1)$$

where i (species in the *trans* compartment) and j (species in the *cis* compartment) represent either different concentrations of MgATP ($z=-2$), or Cl and ATP, respectively, depending on their location on either side of the membrane. The holding potential V_h is in mV, z_i and z_j are the charges for species i and j, respectively, and C_c and C_t are the concentrations of i and j, in either compartment, respectively. P_i and P_j represent the permeability coefficients for either species i or j, respectively. $\alpha = z_i F V_h/RT$ and $\beta = z_j F V_h/RT$, where F, R, and T are Faraday's constant, the gas constant, and absolute temperature, respectively.

The molecular volume of CFTR complexes was calculated as previously described (Schneider et al. 1998), using the equation $V = (\pi h/6)(3r^2 + h^2)$, where h = molecular height and r = the average radius. Whenever indicated, mean data were compared by Student's T-test, and assumed to be statistically different at $P < 0.05$. Data are expressed as mean ± SEM, where n = number of averaged experiments.

Pyrene-actin assay

Fluorescent *N*-(1-pyrenyl)iodoacetamide-labeled actin was obtained from Cytoskeleton (Denver, Colo.), and diluted in monomeric actin at a final concentration of 1 mg/mL in a buffer containing 150 mM KCl and other buffering salts. The rate of actin polymerization was followed by changes in the fluorescence in an Aminco-Bowman spectrofluorometer with excitation and emission wavelengths of 365 and 410 nm, respectively. Once the rate of polymerization reached a quasi-plateau (< 2–3 min), cytochalasin D (5 μg/mL) was added to the cuvette for the remainder of the experiment. Fluorescence was recorded in a chart recorder (Kipp-Zonnen).

Other reagents

Actin, either from Sigma (St. Louis, Mo.) or Cytoskeleton (Denver, Colo.), was stored at a concentration of 0.047 μg/mL stock solution in depolymerizing (G) buffer. The solution contained 0.2 mM $CaCl_2$, 0.2 mM MgATP, 0.2 mM β-mercaptoethanol, and 2 mM Tris-HCl (pH 8.0) until the time of the experiment. Prior to the experiment, actin was further diluted 1:10–100 into the AFM sample volume. Cytochalasin D (Sigma) was kept in DMSO at 1 mg/mL, and added to the test solutions at a final concentration of 5 μg/mL. The monoclonal antibodies MAb no. 13-1 and Mab no. 24-1, raised against the R-domain and the carboxyterminal end of CFTR, respectively, were obtained from Genzyme (Framingham, Mass.). These antibodies were used at a final concentration of 2.92 μg/mL. Whenever indicated, the 13-1 antibody (2.25 mg/mL) was diluted 1:1000 in G buffer and added to the AFM sample. A similar approach was used with the MA 1-935 antibody (Affinity BioReagents, Golden, Colo.), raised against the external epitope peptide GRIIASYDPDNKEER (103–117) of human epithelial CFTR.

Results

Functional reconstitution of CFTR

The effect of various conformations of actin on CFTR function was assessed by functional reconstitution of the channel protein into a lipid bilayer system and determination of ion channel activity as previously reported (Cantiello et al. 1998). The presence of a functional CFTR was first determined in CFTR-containing vesicles. CFTR channel activity was observed in the presence of either 100 and 10 mM MgATP, in the *cis* and *trans* compartments, respectively (Fig. 1A), or asymmetrical Cl (*cis*, 200 mM) and MgATP (*trans*, 10 mM) (Fig. 1B), in agreement with previous findings (Cantiello et al. 1998). Channel activity was observed after addition of PKA (75 nM) to the *cis* chamber. The data indicated that CFTR in the liposomes was functional, allowing the electrodiffusional movement of MgATP, where the apparent permeability in 10 mM ATP was almost ten times that of 100 mM ATP. This is also in agreement with previous studies from our laboratory (Cantiello et al. 1998). The data further suggested that at least some of the channels were oriented as expected from the PKA activation sites on the "cytoplasmic" side of the membrane. Channel activity was also affected by the addition of actin to the *cis* side of the reconstitution chamber. In the presence of PKA, active CFTR channels were inhibited by the addition of a polymerizing concentration of monomeric actin (Fig. 1C). However, addition of short actin polymers, in the form of actin:DNAse I complexes in a 5:1 ratio, readily activated CFTR function. This occurred in the absence of PKA (Fig. 1D). Addition of monomeric actin as actin:DNAse I complexes in a 1:1 ratio, however, reversed the activation effect, inducing CFTR channel inhibition, suggesting that CFTR regulation can be achieved by direct interaction with actin, as suggested by previous reports (Prat et al. 1995).

Effect of CFTR on actin polymerization

As indicated above, the functional data were most consistent with a direct regulatory role of actin on CFTR function. In turn, a CFTR effect on actin polymerization could also be invoked, which was assessed by determining the effect of CFTR-containing vesicles on the actin polymerization process. Changes in

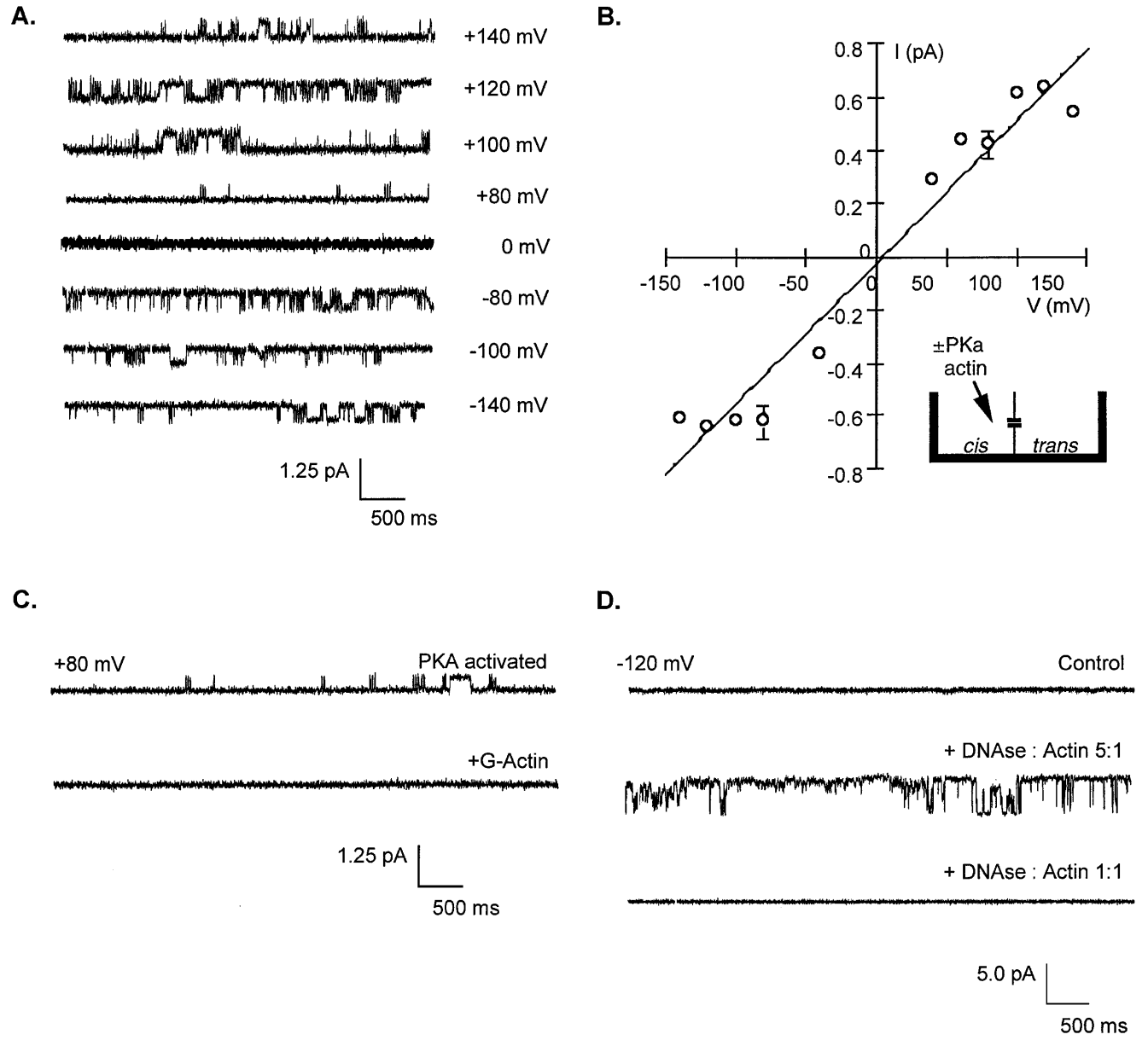

Fig. 1A–D Effect of actin on single-channel currents of reconstituted CFTR. **A** Purified CFTR (in liposomes) was incorporated from the *cis* chamber into a lipid bilayer chamber containing 10 and 100 mM MgATP in the *cis* and *trans*, compartments, respectively. PKA (10 μg/mL) was added to the *cis* chamber to activate CFTR. Both sides of the chamber also contained other buffering compounds (see Materials and methods). Holding potentials were driven from the *trans* chamber; single-channel ATP currents were often observed at positive and negative potentials, as previously reported (Cantiello et al. 1998). Tracings are representative of three experiments. **B** Current-to-voltage relationship of ATP channel currents in asymmetrical MgATP. *Inset*: schematics of the lipid bilayer system. Purified CFTR was always added to the *cis* side of the chamber. Addition of PKA and actin was also carried out from the *cis* chamber. It is expected that activated channels are only presented in one orientation. **C** Addition of G-actin to PKA-activated single ATP channel currents completely inhibited CFTR function. **D** In the presence of Cl, addition of actin:DNAse I at a 5:1 ratio, in the absence of PKA and ATP, stimulated Cl channel activity through reconstituted purified CFTR ($n=3$). Addition of 1:1 actin:DNAse I complexes, however, blocked CFTR channel activity ($n=2$)

fluorescence associated with *N*-(1-pyrenyl)iodoacetamide-labeled actin were followed in a spectrofluorometer. A similar technique was used by Hitt et al. (1994). However, in our studies, the kinetic changes in actin polymerization were followed after addition of cytochalasin D to modify the rate of actin nucleation and polymerization (Goddette and Frieden 1986). After actin polymerization was initiated, addition of cytochalasin D (10 μg/mL) under control conditions (absence of CFTR, Fig. 2A) elicited a rapid increase in fluorescence, which is consistent with a renewed presence of short actin filaments. This effect was observed to be largely reduced in the presence of vesicles containing CFTR (Fig. 2B), but not by vesicles to which CFTR had been exposed to the monoclonal antibody no. 24-1 (Fig. 2C). This is known to interact with a region of CFTR associated with the cytoskeleton in cells (Cantiello 1996).

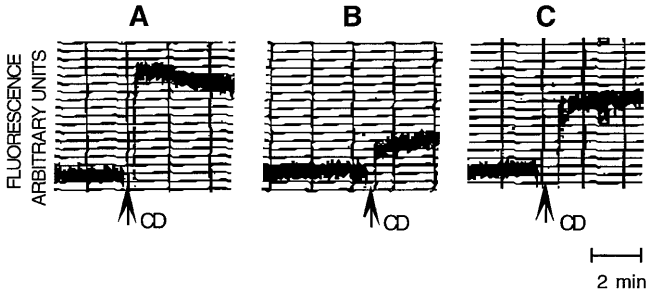

Fig. 2A–C Effect of CFTR on actin polymerization. Fluorescence induced by pyrene-actin was determined in arbitrary units in the absence (**A**) or presence (**B**) of vesicles containing CFTR. CFTR stabilized actin filaments and inhibited the changes elicited by addition of cytochalasin D (5 μg/mL). The effect is largely reversed by addition of Mab no. 24-1 antibody to the CFTR-containing vesicles (**C**). Data represent three different experiments

Atomic force imaging of actin polymerization

Tapping mode AFM was used to image actin filament formation at low concentrations of actin in solution (Fig. 3). Under low ionic strength conditions, namely G buffer, addition of G-actin (~10 nm) elicited the deposition of actin monomers onto the mica surface (Fig. 3a, left), which occasionally formed short actin polymers. The actin monomers aligned into short linear oligomers with an average height of 1.5 ± 0.1 nm ($n = 13$) and a width of 10.4 ± 0.7 nm ($n = 13$, data not shown), which is in agreement with recent studies (Schneider et al. 1998). Actin polymerization in G buffer rapidly increased, however, after addition of KCl to a final concentration of 150 mM (Fig. 3a, right). Double-stranded actin filaments, with a longitudinal pitch of 34.8 ± 1.0 nm, $n = 22$ (Fig. 3b), were observed after polymerization. Similar findings have been previously reported (Fritz et al. 1995).

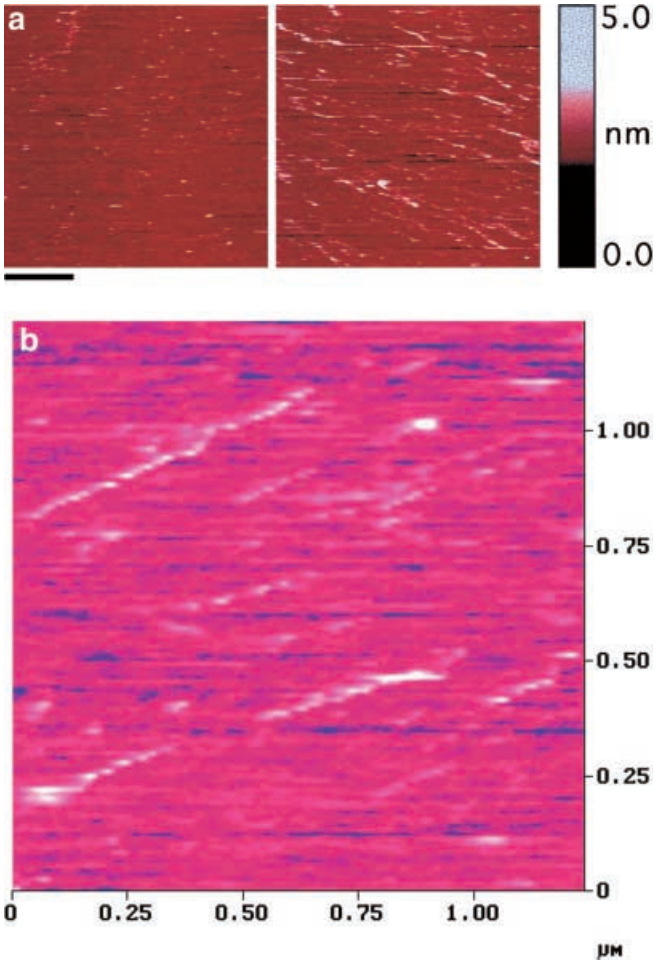

Fig. 3a, b AFM imaging of polymerized actin. **a** *Left*: monomeric actin (0.048 μg/mL) in G buffer was deposited onto the flat surface of freshly cleaved mica. *Right*: actin polymerization was observed within 5 min after addition of a stock KCl solution to final concentration of 150 mM. *Horizontal bar* is 1 μm. **b** Elongated, double-stranded actin filaments can be observed after polymerization with a long pitch of approximately 35–40 nm. Broken down sections of the filaments are also noticeable

Atomic force imaging of CFTR

CFTR-containing liposomes were first imaged under normal pH conditions (7.4), where the round shape and size of the liposome population could be resolved in 2 μm scans (data not shown). Flattened vesicles with an average diameter of 82 nm ($n = 50$) were observed and, occasionally, larger liposomes (> 200 nm diameter) were also observed before flattening. Liposomes fused and flattened either spontaneously, or by "baking" the sample for 1 h at 37 °C. In some cases, a lipid bilayer was formed from liposomes by addition of $MgCl_2$ to a final concentration of 10 mM. The presence of membrane-associated CFTR was manifested in flattened liposomes as protruding spots (Fig. 4, left). Two diameters were commonly distinguished, regardless of the orientation of the proteins (Fig. 4, left, see arrows), which averaged as 36 ± 2 nm ($n = 60$) and 24 ± 1.5 nm ($n = 60$), respectively. An average height of 1.90 ± 0.1 nm ($n = 60$) was determined regardless of orientation and diameter. Addition of the monoclonal antibody (MAb no. 13-1), raised against the cytoplasmic "R-domain" of the channel, changed the size of the protruding protein and induced a 1.1 ± 0.5 nm ($n = 22$) increase in the height of the complex (data not shown).

Actin interaction(s) with CFTR

To determine whether actin directly interacts with CFTR, flattened CFTR-containing liposomes were first scanned and G-actin (10 nM) was added to the liquid sample. Higher resolution scans were then conducted between 1–10 min after addition. Actin filaments were observed extending from CFTR (Fig. 5A). CFTR molecules were further identified by addition of either external epitope or intracellular R-domain specific antibodies (Fig. 5B–D). Little or no actin polymerization

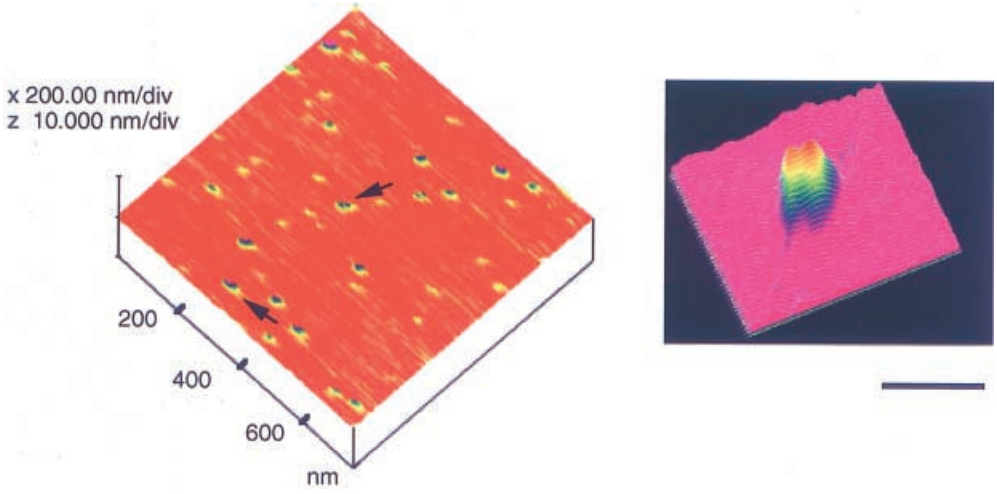

Fig. 4 AFM imaging of CFTR. *Left*: a field of protruding molecules was observed by a 3D perspective of images. For analysis, linear parameters were measured in "*x*" and "*y*" axes, regardless of orientation, as indicated by the *arrows*. *Right*: higher resolution scans were also conducted on flattened liposomes. CFTR molecules were resolved with an average diameter of approximately 30 nm and 1.9 nm in height. *Horizontal bar* indicates 50 nm

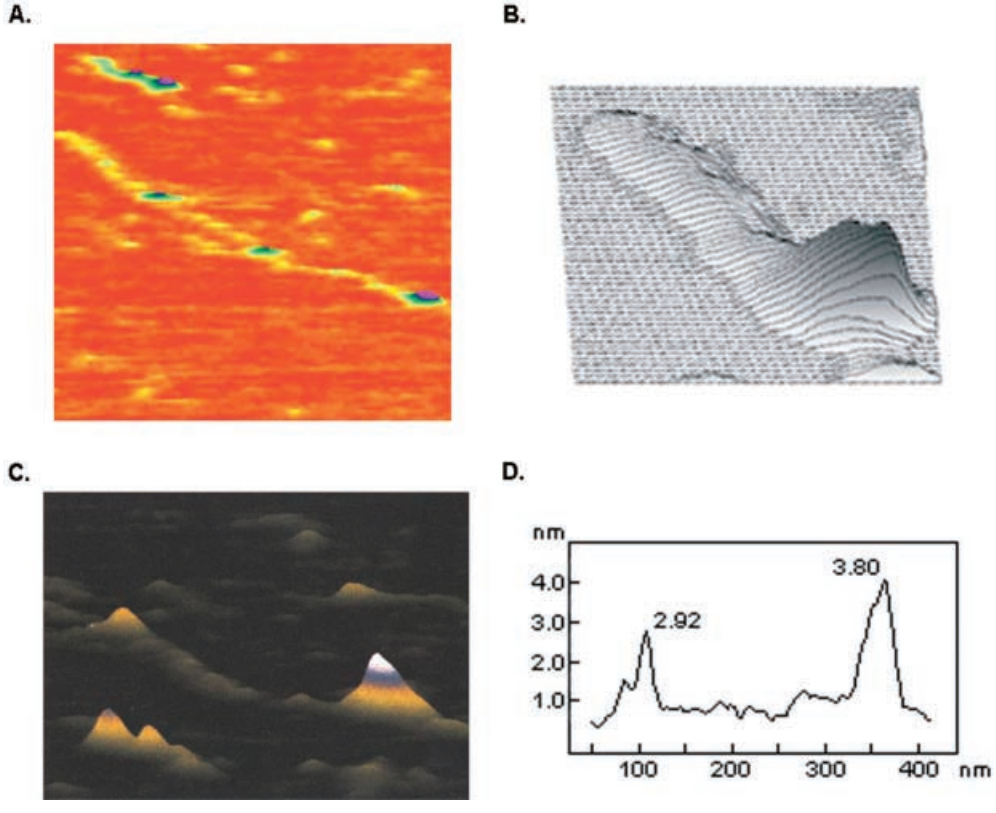

Fig. 5A–D Actin interactions with CFTR. **A** Monomeric actin (0.048 μg/mL) in G buffer, also containing 150 mM KCl, elongated into actin filaments (*yellow*), spontaneously aligning between CFTR molecules. **B** CFTR served as a nucleating factor for actin elongation. **C** Image of actin bundles associated with CFTR molecules. CFTR on *bottom right* is topped with an anti-CFTR antibody (*white*). **D** Histogram of dimensional properties of actin filaments connected to CFTR molecules. The higher CFTR molecule is associated with an anti-CFTR antibody

was observed detached from CFTR molecules (Fig. 5C), suggesting that the transmembrane channel structure promotes actin assembly, where actin monomers elongated from the CFTR molecules.

Discussion

The main goal of the present study was to assess a physical interaction between actin and CFTR. The data in this report indicate that CFTR directly interacts, and likely promotes the polymerization (nucleation) of actin monomers, as observed by the imaging of the two proteins by AFM. A physical interaction between actin and CFTR provides a suitable explanation for the regulation by actin of CFTR function previously reported (Prat et al. 1995, 1999). CFTR regulation by the actin cytoskeleton is carried out, at least partly, by actin itself. Further evidence for a functional interaction is our finding that actin modified CFTR function of the purified reconstituted channel protein, and conversely, that CFTR may actually change the rate of actin polymerization.

Tapping mode AFM in aqueous environments has provided information on a variety of cell components,

including the cell's cytoskeleton (Radmacher et al. 1992; Fritz et al. 1995; Rotsch and Radmacher 2000). Previous AFM studies have also provided evidence on the topology of actin filaments in saline solution (Weisenhorn et al. 1990; Fritz et al. 1995). However, imaging of actin filaments in vitro, and/or the actual process of actin polymerization, has been difficult (Fritz et al. 1995), in particular because the lability with which actin structures interact with the substrate surface. Our ability to identify the formation of isolated actin filaments in solution may lay in the fact that actin was allowed to deposit in the monomeric state and undergo surface polymerization. The structures observed had the topological features consistent with previous reports. Nevertheless, the actin filaments formed in normal saline solution were indeed labile and easily broken, likely by the interaction with the stylus. In studies (to be published elsewhere), we have found that actin filaments are more robust in the presence of increased concentrations of divalent cations, and also in the presence of actin binding proteins.

To date, only a few transmembrane proteins including the ion channels OmpF porin (Mueller et al. 1997) and RomK1 (Oberleithner et al. 1997), as well as bacteriorhodopsin (Butt et al. 1990) and the FoF1ATP synthase (Neff et al. 1997), have been imaged by AFM. In this report, CFTR molecules were imaged by scanning flattened liposomes containing the channel protein. To obtain an estimate of the CFTR volume, the "x" and "y" axes were averaged. This would take into account the distinct resolution in directional axes. An average spherical radius of approximately 15 nm and a height of 2 nm were calculated. Assuming that the extramembrane volume is the cap of a sphere, a protruding volume of 675 nm^3 can be calculated, rendering an extramembrane molecular mass of the order of 320 kDa (Schneider et al. 1998). This very rough estimate is to be compared with the mass of the monomer, 162 kDa. These calculations do not take into account intramembrane volume. Interestingly, similar results have been reported by other groups on topologically similar proteins.

The molecular topology of two members of the ABC family of transporters, namely P-glycoprotein and HisP, has recently been determined by transmission electron microscopy and X-ray diffraction, respectively (Rosenberg et al. 1997; Hung et al. 1998). The calculated size of the HisP dimer was 340 nm^3 (Hung et al. 1998), consistent with a molecular complex of approximately 90 kDa, instead of its expected monomeric value, 52 kDa. Similarly, the molecular reconstruction of P-glycoprotein, with a molecular weight of 170 kDa, rendered a cylindrical structure of 10 nm diameter and 8 nm height (Rosenberg et al. 1997). The authors calculated a molecular mass of 540 kDa, assuming 0.7 cm^3/g. This is twice as large as the monomer's expected size. Thus, all three ABC transporters, including CFTR, yield mass estimates consistent with a molecular complex twice as large as those expected for monomers. Whether this phenomenon is due to either dimer formation or a very loosely packed monomer (Rosenberg et al. 1997) will require further experimentation.

The present study indicates that structural as well as functional interfaces essential for channel activation, including the cAMP-mediated CFTR response (Prat et al. 1995), may rely on a physical interaction between actin and CFTR. The data also suggest that various actin conformations may modify the conformational states of CFTR, even in the absence of PKA. This contention will require further investigation. However, putative actin binding domains have been suggested in both nucleotide binding folds of CFTR (Prat et al. 1995), thus supporting the working hypothesis that actin, which binds directly to CFTR, may change conformations, and in turn, cause conformational changes to the channel protein.

Acknowledgements The authors are grateful to Mrs. Anlee Krupp of the Microanalysis facility of the Boston University Photonics Center for invaluable advice and assistance with instrumentation and to Nathan D. Burns for excellent technical support. K.P. was supported by the Boston University Summer Internship Program (1999). N.A.G. was supported in part by the Boston University Undergraduate Research Opportunities Program.

References

Alvarez O (1986) How to set up a bilayer system. In: Alvarez O (ed) Ion channel reconstitution. Plenum Press, New York, pp 115–130

Berger HA, Anderson MP, Gregory RJ, Thompson S, Howard PW, Maurer RA, Mulligan R, Smith AE, Welsh MJ (1991) Identification and regulation of the cystic fibrosis transmembrane conductance regulator-generated chloride channel. J Clin Invest 88:1422–1431

Binnig G, Quate CF, Gerber C (1986) Atomic force microscope. Phys Rev Lett 56:930–934

Butt H-J, Downing KH, Hansma PK (1990) Imaging the membrane protein bacteriorhodopsin with the atomic force microscope. Biophys J 58:1473–1480

Cantiello HF (1996) Role of the actin cytoskeleton in the regulation of the cystic fibrosis transmembrane conductance regulator. Exp Physiol 83:505–514

Cantiello HF, Jackson GR Jr, Grosman CF, Prat AG, Borkan SC, Wang Y-H, Reisin IL, O'Riordan CR, Ausiello DA (1998) Electrodiffusional ATP movement through the cystic fibrosis transmembrane conductance regulator. Am J Physiol 274:C799–C809

Drake B, Prater CB, Weisenhorn AL, Gould SAC, Albrecht TR, Quate CF, Cannell DS, Hansma HG, Hansma PK (1989) Imaging crystals, polymers, and processes in water with the atomic force microscope. Science 243:1586–1588

Fritz M, Radmacher M, Cleveland JP, Allersma MW, Stewart RJ, Gieselmann R, Janmey P, Schmidt CF, Hansma PK (1995) Imaging globular and filamentous proteins in physiological buffer solutions with tapping mode atomic force microscopy. Langmuir 11:3529–3535

Goddette DW, Frieden C (1986) The kinetics of cytochalasin D binding to monomeric actin. J Biol Chem 261:15970–15973

Hitt AL, Lu TH, Luna EJ (1994) Ponticulin is an atypical membrane protein. J Cell Biol 126:1421–1431

Hung L-W, Wang IX, Nikaido K, Liu P-Q, Ferro-Luzzi Ames G, Kim S-H (1998) Crystal structure of the ATP-binding subunit of an ABC transporter. Nature 396:703–707

Hurley J (1996) The sugar kinase/heat-shock protein 70/actin superfamily: implications of conserved structure for mechanism. Annu Rev Biophys Biomol Struct 25:137–162

Mueller DJ, Schoenenberger C-A, Schabert F, Engel A (1997) Structural changes in native membrane proteins monitored at subnanometer resolution with the atomic force microscope: a review. J Struct Biol 119:149–157

Neff D, Tripathi S, Middendorf K, Stahlberg H, Butt H-J, Bamberg E, Dencher NA (1997) Chloroplast FoF1ATP synthase imaged by atomic force microscopy. J Struct Biol 119:139–148

Oberleithner H, Schneider S, Henderson R (1997) Structural activity of a cloned potassium channel (ROMK1) monitored with the atomic force microscope: the ''molecular-sandwich'' technique. Proc Natl Acad Sci USA 94:14144–14149

O'Riordan C, Erickson A, Bear C, Li C, Manavalan P, Wang K, Marshall J, Scheule R, McPherson J, Cheng S, Smith A (1995) Purification and characterization of recombinant cystic fibrosis transmembrane conductance regulator from Chinese hamster ovary and insect cells. J Biol Chem 270:17033–17043

Prat AG, Xiao Y-F, Ausiello DA, Cantiello HF (1995) cAMP-independent regulation of CFTR by the actin cytoskeleton. Am J Physiol 268:C1552–C1561

Prat AG, Cunningham CC, Jackson GR Jr, Borkan SC, Wang Y, Ausiello DA, Cantiello HF (1999) Actin filament organization is required for proper cAMP-dependent activation of CFTR. Am J Physiol 277:C1160–C1169

Radmacher M, Tillmann RW, Fritz M, Gaub HE (1992) From molecules to cells: imaging soft samples with the AFM. Science 257:1900–1905

Rich DP, Anderson MP, Gregory RI, Cheng SH, Paul S, Jefferson DN, McCann ID, Klinger KW, Smith AE, Welsh MJ (1990) Expression of cystic fibrosis transmembrane conductance regulator corrects defective chloride channel regulation in cystic fibrosis airway epithelial cells. Nature 347:358–363

Rosenberg MF, Callaghan R, Ford RC, Higgins CF (1997) Structure of the multidrug resistance P-glycoprotein to 2.5 nm resolution by electron microscopy and image analysis. J Biol Chem 272:10685–10694

Rotsch C, Radmacher M (2000) Drug-induced changes of cytoskeletal structure and mechanics in fibroblasts: an atomic force microscopy study. Biophys J 78:520–535

Schneider S, Larmer J, Henderson R, Oberleithner H (1998) Molecular weights of individual proteins correlate with molecular volumes measured by atomic force microscopy. Pflügers Arch 435:362–367

Short D, Trotter K, Reczek D, Kreda S, Bretscher A, Boucher R, Stutts M, Milgram S (1998) An apical PDZ protein anchors the cystic fibrosis transmembrane conductance regulator to the cytoskeleton. J Biol Chem 273:19797–19801

Strickland E, Bao-He Q, Millen L, Thomas PJ (1997) The molecular chaperone Hsc70 assists the in vitro folding of the N-terminal nucleotide-binding domain of the cystic fibrosis transmembrane conductance regulator. J Biol Chem 272:25421–25424

Weisenhorn AL, Drake B, Prater CB, Gould SAC, Hansma PK, Ohnesorge F, Egger M, Heyn SP, Gaub HE (1990) Immobilized proteins in buffer imaged at molecular resolution by atomic force microscopy. Biophys J 58:1251–1258